Report Advanced Laboratory

October 28, 2020

1 Introduction

We consider the electron-positron scattering with muon-antimuon threshold production along a Beryllium block, studying its cross section and properties of the outgoing muon beam. We present an algorithm for reconstructing the trajectory of the muons emerging from a magnetic field region.

2 Muons production in Beryllium

2.1 Theory

We consider the scattering event

$$e^+ + e^- \to \mu^+ + \mu^-. \tag{1}$$

We start by computing the leading-order cross section $\sigma(\theta, \sqrt{s})$ as a function of the scattering angle θ and the center of mass energy $\sqrt{s}$. In the center of mass (CM) frame we obtained

$$\frac{d\sigma}{d\Omega}(\theta, \sqrt{s}) = \frac{\alpha^2}{4s}\sqrt{\frac{1-(m_\mu^2/s)}{1-(m_e^2/s)}}\left[1+4\frac{m_e^2+m_\mu^2}{s}+\left(1-\frac{4m_e^2}{s}\right)\left(1-\frac{4m_\mu^2}{s}\right)\cos^2\theta\right] \tag{2}$$

where $\alpha \simeq \frac{1}{137}$ is the fine-structure constant and m_e, m_μ are the electron and the muon masses.
In the CM frame the energy E^* and momentum p^* of the emerging muon pairs are

$$E^* = \frac{\sqrt{s}}{2}, \qquad p^* = \sqrt{\frac{s}{4} - m_\mu^2}\,. \tag{3}$$

On the other hand, the CM velocity β and the Lorentz factor γ are (with respect to the laboratory)

$$\beta = \sqrt{1-\frac{4m_e^2}{s}}, \qquad \gamma = \frac{\sqrt{s}}{2m_e}. \tag{4}$$

Performing a Lorentz boost along the z-axis gives

$$E = \gamma(E^* + \beta p_z^*), \qquad p_z = \gamma(p_z^* + \beta E^*), \qquad p_x = p_x^*, \qquad p_y = p_y^*. \tag{5}$$

2.2 Implementation

2.3 Collision depth probability

To compute the probability that the collision takes place at a depth z inside the target, we discretized the target into small intervals of length $dz = 30\mu m$. When the positron crosses the i^{th} interval it has a probability of generating muons

$$dp_i = n\sigma(\sqrt{s_i})dz \tag{6}$$

where n is the target electron density and the cross section is computed assuming that the energy of the beam in the laboratory frame decays exponentially.

$$E_i = E_0 e^{-\frac{idz}{X_0}} \Rightarrow s_i = 2m_e(E_i + m_e) \tag{7}$$

where $X_0 = 0.3528\ m$ is the radiation length of beryllium. We compute the probability of having an interaction in the i^{th} interval as

$$P(z = idz) = \prod_{j<i}(1 - dp_j)dp_i \tag{8}$$

approximating the process as Bernouillian.

2.4 Event simulation

The simulation of each event consists in the following steps.

- The energy of the incident positron is chosen following a gaussian distribution with $\mu_E = 49\ GeV; \sigma_E = 0.5\ GeV$. We choose these values so that also the positrons $6\sigma_E$ below the average energy have the possibility to produce muons for the whole length of the target

$$E_0 \geq \frac{2m_u^2}{m_e} e^{d/X_0} = 45GeV. \tag{9}$$

- Sampling the position of interaction with a pdf that follows the behavior of (8) renormalized on the target total length.
- Computing the energy of the energy of the beam relative to the selected position z and the corresponding value of s.
- Selecting the angles in the center of mass frame following the distribution (2) and compute the relative quadri-momenta of the muons.
- We boost the obtained values to pass to the laboratory frame.
- Generating independently offset on x and y
- Generating independently angles of divergence of the positron beam, α around the x axis and β around the y one. We then rotate the generated momenta around the point of scattering to account for the divergence of the beam as follows.

$$\begin{pmatrix} p'_x \\ p'_y \\ p'_z \end{pmatrix} = \begin{pmatrix} cos(\beta) & 0 & sin(\beta) \\ sin(\alpha)sin(\beta) & cos(\alpha) & -cos(\beta)sin(\alpha) \\ -cos(\alpha)sin(\beta) & sin(\alpha) & cos(\alpha)cos(\beta) \end{pmatrix} \begin{pmatrix} p_x \\ p_y \\ p_z \end{pmatrix}$$

2.5 Experimental results

We computed the cross section along the $3cm$ block. For our beam mean energy of $\mu_E = 49\,GeV$ the probability of the muon production increases along the block. As shown in Figure 1.

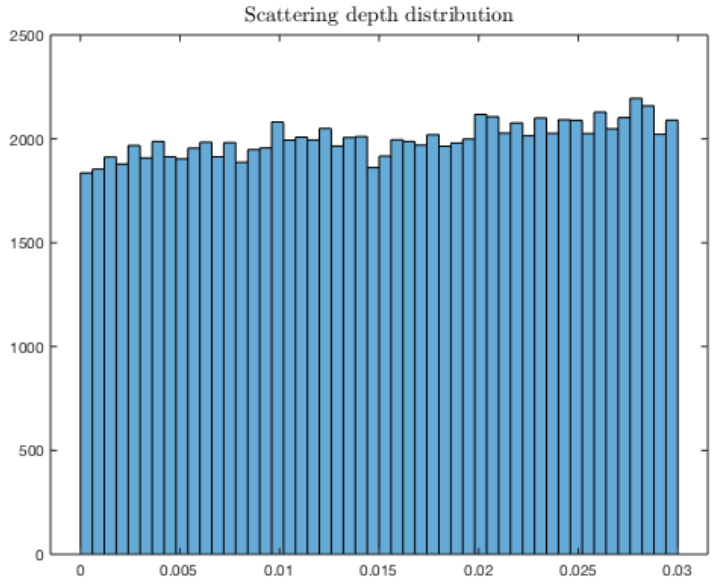

Figure 1: Number of events generated as a function of the depth z.

The physical meaning of this result originates from Equation 2, in which one can see that $\frac{d\sigma}{d\Omega} \propto \frac{1}{s}$. Since we expect that in the beryllium block the energy decreases exponentially, the differential cross section must increase. In the following we report the momenta distributions of the produced muons along the block.

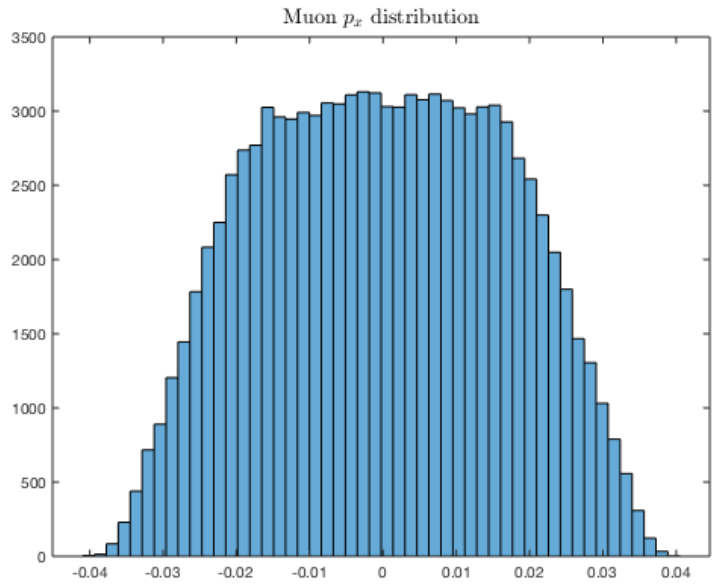

Figure 2: Number of events generated as a function of the momentum along the x-axis p_x.

Due to the symmetry of the system, the events in function of the momentum along the y-axis p_y exhibit the same distribution. As expected, Figure 2 shows a distribution symmetrical around zero.

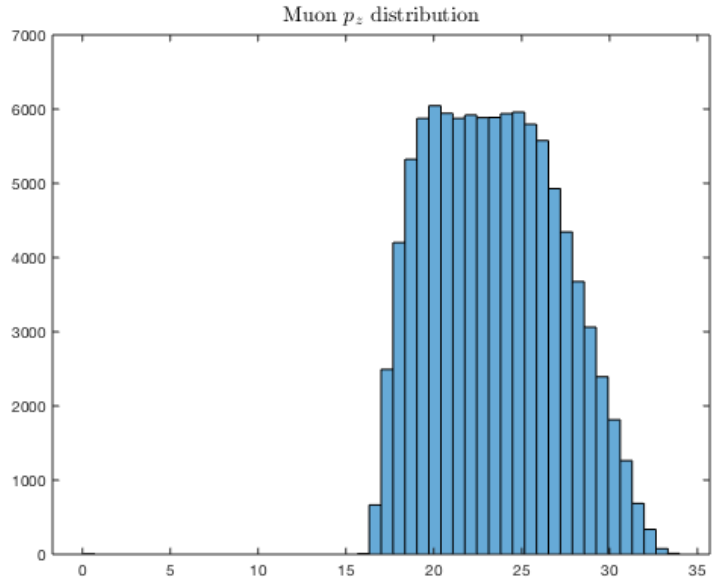

Figure 3: Number of events generated as a function of the momentum along the z-axis p_z.

Figure 3 shows an asymmetrical distribution, due to the fact that the probability distribution of having an event at depth z is not uniform. As said before, in general we expect that the probability of having an event is roughly proportional to the depth z, so it is reasonable to record more events at lower p_z.

For completeness we have computed the angles of each event with respect to the z-axis, in order to have an idea of the divergence of the beam. In Figure 4 we have considered an initial positron beam without an intrinsic divergence.

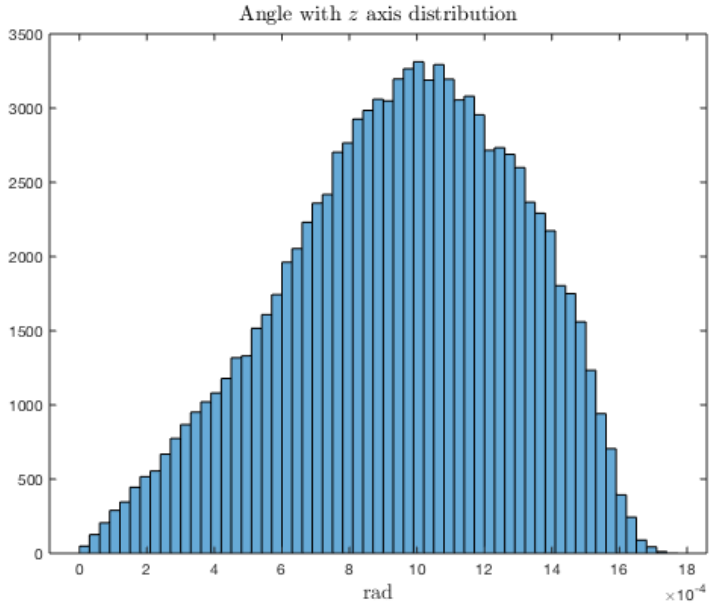

Figure 4: Number of events as function of the angle with respect to the z-axis.

In Figure 5 instead, we have considered an initial positron beam with a certain intrinsic divergence.

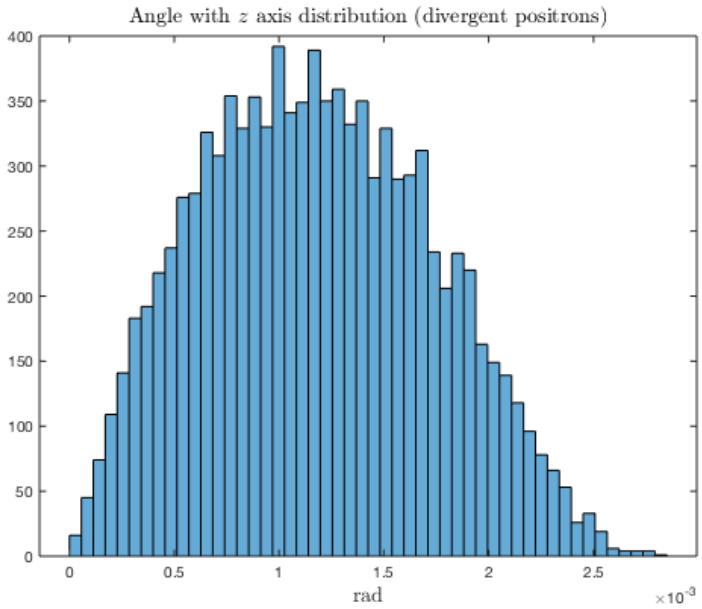

Figure 5: Number of events as function of the angle with respect to the z-axis, including an initial divergence for the positron beam.

2.6 Acquisition time estimation

The probability for a positron to collide and produce muons can approximately be estimated as

$$P = n\sigma\Delta z \simeq 3.5 \cdot 10^{-6} \tag{10}$$

where n is the electron density of beryllium, Δz the thickness of the target and σ is evaluated for an incident particle with energy $E = 49\ GeV$. The positrons hits the target with a frequency of 1 MHz so, muons have a production rate about 3.5 s^{-1}. Assuming an almost unitary efficiency of the detection system, if we want to acquire a set with $\sim 10^5$ events an observation of about 8 hours is required.

3 Trajectory reconstruction

3.1 Hit dataset generation

We model a particle with momentum $\begin{pmatrix} p_x, & p_y, & p_z \end{pmatrix}^\top$ and whose trajectory passes through point $\begin{pmatrix} x, & y, & z \end{pmatrix}^\top$ as a vector $\boldsymbol{t} = \begin{pmatrix} x, & y, & z, & p_x, & p_y, & p_z \end{pmatrix}^\top$. Then, we model a particle detector as a rectangle perpendicular to the z-axis and with center lying on the z axis, with configurable height, width and z position. Given a particle trajectory $\boldsymbol{t}$ and a detector at position z_0, the position of the simulated hit is hence

$$\begin{pmatrix} x + \frac{p_x}{p_z}(z_0 - z) \\ y + \frac{p_y}{p_z}(z_0 - z) \\ z_0 \end{pmatrix} + \boldsymbol{\eta}, \qquad \vec{\eta} \sim \mathcal{N}\left(\vec{0}, \begin{pmatrix} \sigma_x & 0 & 0 \\ 0 & \sigma_y & 0 \\ 0 & 0 & 0 \end{pmatrix}\right), \tag{11}$$

where $\boldsymbol{\eta}$ is the noise from the background. Then for each event provided by the user, which is a collection of three vectors $\boldsymbol{t}$ (one for the incoming positron and two for the emerging muons), the software produces a collection of hits, each represented as a point in space. If requested false positives can be added to the data; their number on each detector is distributed as a Poisson(λ). False positives events are distributed uniformly over the area of the detector.

3.2 Trajectory reconstruction

We proceed to describe the algorithm for reconstructing the trajectory of a particle given the produced hits.
Firstly, the algorithm computes the trajectory $\overline{\mathbf{t}} = \begin{pmatrix} \bar{x}, & \bar{y}, & 0, & p_x/p_z, & p_y/p_z, & 1 \end{pmatrix}^\top$ and then it reconstructs the momentum from the trajectory deviation (due to the magnetic field) to produce the full description $\boldsymbol{t}$ of the particle. Consider a vector of detectors with positions $z^{(1)}$, ..., $z^{(m)}$, then the vector of the x component of the hits is describe by the linear model

$$\mathbf{v}_x = \begin{pmatrix} 1 & z^{(1)} \\ 1 & z^{(2)} \\ \vdots & \vdots \\ 1 & z^{(m)} \end{pmatrix} \begin{pmatrix} \bar{x} \\ p_x/p_z \end{pmatrix} + \boldsymbol{\eta} =: \Phi\theta_{\mathbf{x}} + \boldsymbol{\eta}. \tag{12}$$

The same holds for the y component $\mathbf{v}_y$.
We choose the maximum likelihood estimator as our estimator

$$\hat{\theta} = \arg\max_{\theta} \mathbb{P}(\theta \mid \mathbf{v}) = \arg\max_{\theta} \mathbb{P}(\mathbf{v} \mid \theta)\mathbb{P}(\theta) \simeq \arg\max_{\theta} \mathbb{P}(\mathbf{v} \mid \theta). \tag{13}$$

Let

$$\Sigma_x = \begin{pmatrix} \sigma^2_{(1)} & 0 & \dots & 0 \\ 0 & \sigma^2_{(2)} & \dots & 0 \\ \vdots & \vdots & \ddots & \vdots \\ 0 & 0 & ... & \sigma^2_{(m)} \end{pmatrix} \tag{14}$$

be the covariance matrix of the gaussian noise on the x component. Since the model is gaussian and linear we have that, by the Gauss-Markov theorem,

$$\hat{\theta}_x = \left(\Phi^\top \Sigma^{-1} \Phi\right)^{-1} \Sigma^{-1} \Phi^\top \mathbf{v_x} \tag{15}$$

and

$$\mathrm{Cov}(\hat{\theta}_x) = \left(\Phi^\top \Sigma^{-1} \Phi\right)^{-1} \ . \tag{16}$$

For typical settings of this experiment we have $m = 4$, $\Sigma = \sigma^2 \mathbb{I}$ with $\sigma^2 \simeq 10^{-8} m^2$ and $0 \leq z^{(i)} \leq 10m$. Hence $\sigma(\bar{x}) \simeq 10^{-4} m$ and $\sigma(p_x/p_z) \simeq 10^{-5}$. For typical values of $\bar{x}$ and p_x/p_z we have

$$\frac{\sigma_{\bar{x}}}{\bar{x}} \simeq 10^{-2}, \qquad \frac{\sigma_{p_x/p_z}}{p_x/p_z} \simeq 10^{-2} \ . \tag{17}$$

We now deal with the false positives. Let m be the number of detectors of interest and let $\mathfrak{h}_1, \mathfrak{h}_2, ..., \mathfrak{h}_m$ be the number of hits on each detector (false positive included). Then we have $\prod_{i=1}^m \mathfrak{h}_i$ ways to choose one hit for each detector. For each choice we use the least squares fit described above to get an estimate for the values of $\bar{x}$, $\bar{y}$, p_x/p_z and p_y/p_z and hence an estimate $\hat{\mathbf{t}}$ for the vector $\bar{\mathbf{t}}$. Let $\mathbf{h}_i(\hat{\mathbf{t}})$ be the hit of trajectory $\bar{\mathbf{t}}$ on the i-th detector (without any smearing). For each estimate we then compute its likelihood

$$\mathbb{P}(\mathbf{v} \mid \hat{\mathbf{t}}) \propto \prod_{i=1}^{m} \exp\left\{-\|\mathbf{h}_i(\hat{\mathbf{t}}) - \mathbf{v}^{(i)}\|^2\right\}$$

where $\mathbf{v}^{(i)} = (\mathbf{v}_x^{(i)}, \mathbf{v}_y^{(i)}, z^{(i)})$. Then, we choose the subset of hits with highest likelihood (or the best two in the case of muon trajectories).

3.3 Momentum measure

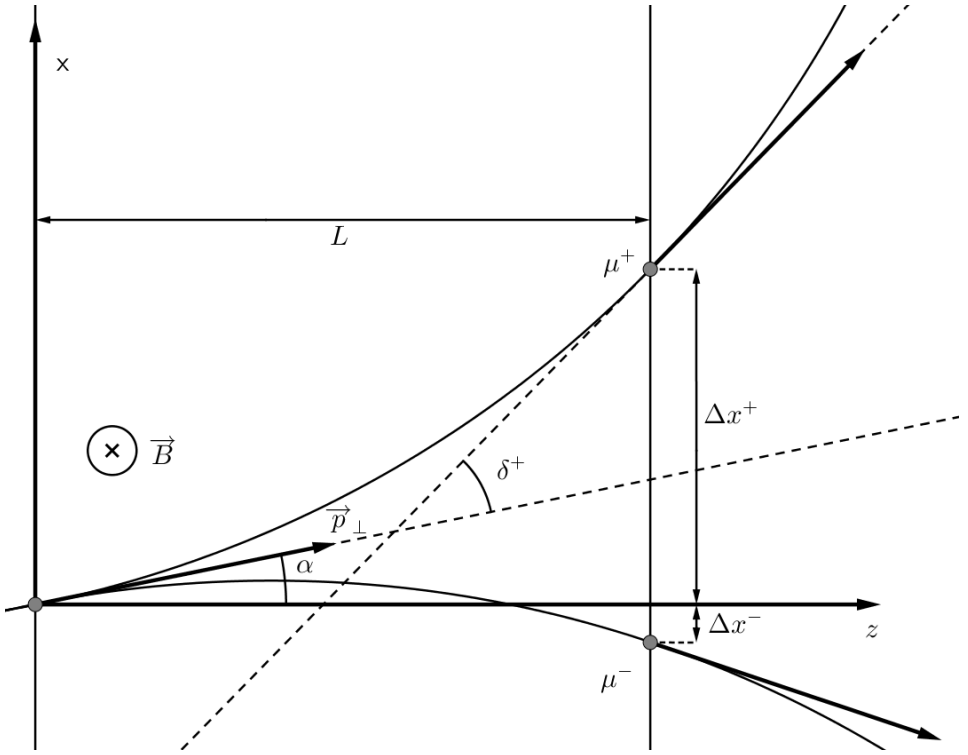

Figure 6: Sketch of the muons' trajectories in the magnetic field.

The muons cross a region of length $L = 2m$, where there is a uniform magnetic field $\mathbf{B} = -B\hat{y}$, $B = 1.7T$. In the xz-plane the muons trajectory is deviated by an angle $\delta^\pm$ depending on their charge sign. Considering a particle entering the region with momentum $\mathbf{p} = (p_x, p_y, p_z)^\top$, we introduce the notation

$$p_\perp = \sqrt{p_x^2 + p_z^2}, \qquad R = \frac{p_\perp}{qB}, \qquad \alpha = \tan^{-1}\left(\frac{p_x}{p_z}\right). \tag{18}$$

We consider $R < 0$ for negative particles.
The position and momentum of a particle when it exits the field can be calculated in the xz-plane from the intersections of the circumference of the trajectory projection and the line $z = L$

$$\begin{cases} \Delta x^\pm = R\cos\alpha \mp \sqrt{R^2 - (L + R\sin\alpha)^2} \\ \Delta z = L \end{cases},$$

$$\begin{cases} p_x'^\pm = \pm p_\perp \sin\left(\tan^{-1}\left(\frac{L+R\sin\alpha}{\sqrt{R^2-(L+R\sin\alpha)^2}}\right)\right) \\ p_z' = p_\perp \cos\left(\tan^{-1}\left(\frac{L+R\sin\alpha}{\sqrt{R^2-(L+R\sin\alpha)^2}}\right)\right) \end{cases}. \tag{19}$$

Thus, the deviation angle results

$$\delta^\pm = \cos^{-1}\left(\frac{p_x p_x'^\pm + p_z p_z'}{p_\perp^2}\right) \tag{20}$$

and the uniform motion along the y-axis gives

$$\Delta y = |R\delta^{\pm}|\frac{p_y}{p_\perp}, \qquad p'_y = p_y. \tag{21}$$

We used the above formulas to calculate the deviation of simulated trajectories. Experimentally, we measured the lines along which the particle moves before and after the magnetic field region. From those we can calculate the displacement $\mathbf{\Delta} = (\Delta x, \Delta y, \Delta z)^\top$ and the deviation angle δ from the scalar product of the versors of the two directions in the xz-plane

$$|\delta| = \cos^{-1}(\hat{p}_{(xz)} \cdot \hat{p}'_{(xz)}).s \tag{22}$$

We can invert the previous relations to calculate the particle momentum from the measured data defining

$$d = \sqrt{\Delta x^2 + \Delta z^2} \Rightarrow |R| = \frac{d}{2\sin(\delta/2)}, \tag{23}$$

we have

$$p_\perp = |qR|B, \qquad p_y = \frac{p_\perp \Delta y}{|R\delta|}, \qquad p = \sqrt{p_\perp^2 + p_y^2}\,. \tag{24}$$

The direction of the momentum is the one of the line that fits the hits on detectors before the field. We assume that in the production process the electron is at rest and so we calculate the momentum of the positron as the sum of the momenta of the two muons

$$\mathbf{p}_{e^+} = \mathbf{p}_{\mu^+} + \mathbf{p}_{\mu^-}. \tag{25}$$

Since in the simulation we know the true value of the momentum for each event we define the quantity

$$\epsilon = \log_{10}\left(\frac{|\mathbf{p}_m - \mathbf{p}_r|}{|\mathbf{p}_r|}\right) \tag{26}$$

where $\mathbf{p}_m$ and $\mathbf{p}_r$ are respectively the measured value of positron momentum and the real one. We will use the distribution of this quantity for the next analysis.

3.4 Trajectory matching

Since the muons are generated as pairs, we have two incoming lines and two outcoming ones for each event. The first criterium we used to match trajectories exploit the conservation of the momentum along the y-axis. For this reason, we match the line with the greater component along y-axis before the field with the one with the greater component after the field. This method however fails for events that occur almost in the xz-plane since the error in the direction measurement can lead to a wrong coupling. In our simulation this error occurs with a frequency of about 1 %. In those cases, the difference with respect to the real total momentum permits to identify the error as we can see from Figure 7 where the errors populates the low right-tale part of the histograms. In the experiment, however, the real value is unknown and errors

of this kind can't be so easily identified, due to the variability in the initial positron momentum. In our simulation, we started by considering that all positrons collide on the target with momentum along the z-axis. To identify the correct match we can try both possibilities and select the one in which the total momentum is less inclined with respect to the z-axis. With this second criterium, however, we still get a 2% error rate. Combining the two criteria and discarding events in which they give different results, if we assume the two tests are independent, the fraction of undetected errors should drop to 0.02%. The fraction of discarded events is about 3%. The implementation of the second criterium , however, requires a good knowledge of the direction of motion of the positron that needs to be measured with detectors in front of the target. We also tried a hybrid method in which we set a threshold on the minimum inclination of muons trajectories in the yz-plane above which we use the first criteria, or we use the second otherwise. With this method the error rate reduces to 0.3%.

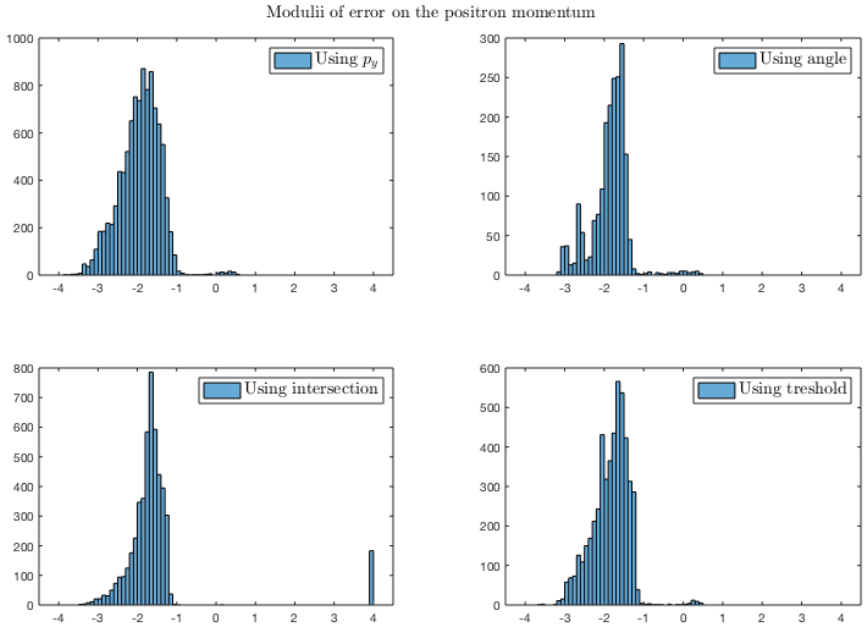

Figure 7: ϵ distribution obtained with the four different methods

Finally we tried a different implementation of the first criteria which results to be the most efficient. In this case for each line, we calculate the sum of the y position of the corresponding hit on the detectors and we match the two with the greater sum. The error rate of this method results 0.2%. Figure 8 shows the distribution of ϵ with this method.

Figure 8: ϵ distribution

3.5 Setup geometry

To determine the positions and sizes of the detectors we looked at the simulated trajectories. Figure 9 shows the distribution of the angle θ_{xz}, in the xz-plane, between the trajectory and the z-axis. The two different distributions show that the magnetic field separates the positive and negative particles into two different beams.

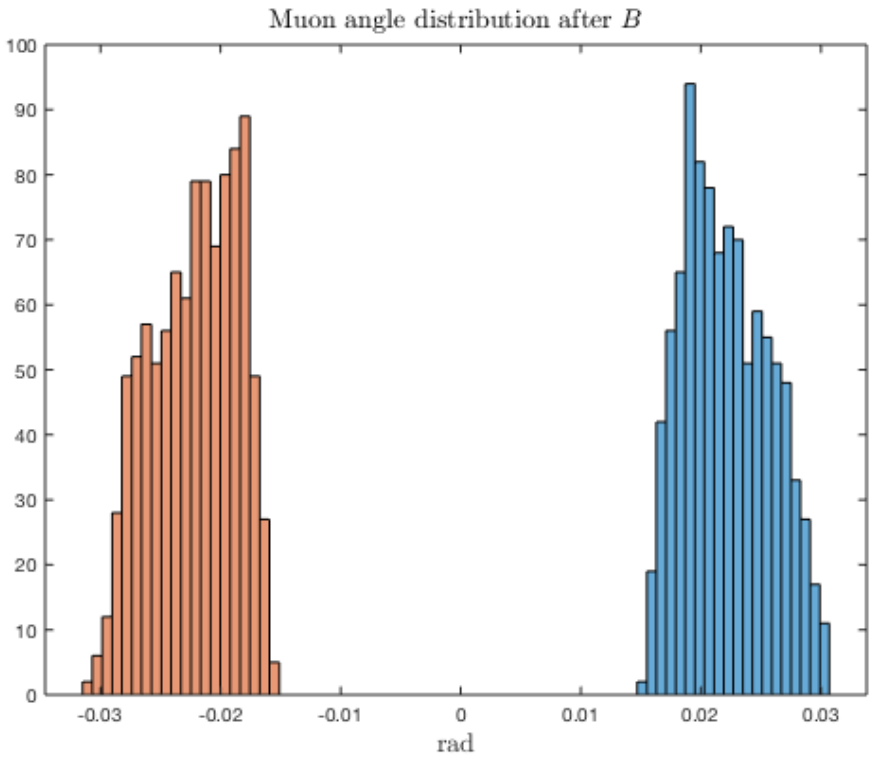

Figure 9: Muons distribution after the magnetic field. In the horizontal axis we have the angle in the xz-plane with respect to the z-axis.

We evaluated the distribution of ϵ (see Equation 26) both in the case where we use detectors to track the incoming positrons and in the case we just calculate its momentum as the sum of the two muons. Figure 10 shows that the results are similar in both cases, so we decided to avoid putting detectors before the target.

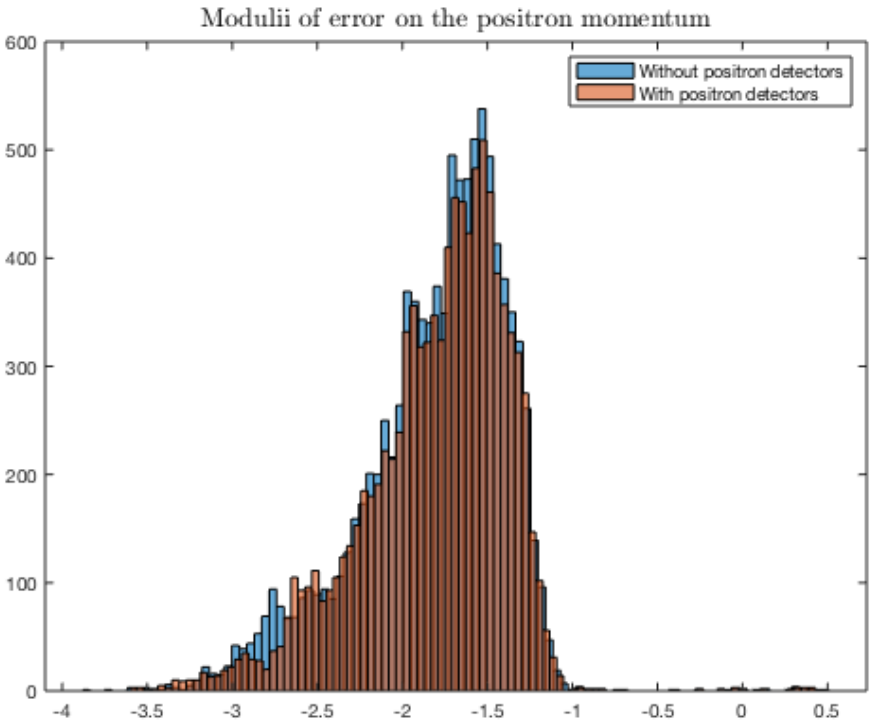

Figure 10: ϵ distribution. Comparison between the two tracking approaches, with or without positron detection.

Now, let us consider a setup where there are m detectors before the magnetic field and m pairs of detectors after the field. Figure 11 shows how the distribution of ϵ changes for $m = \{3, 4, 5\}$. We can see that choosing $m = 4$ for almost all events the relative error is below 10% while the case $m = 5$ doesn't show much improvement. So we foresee a setup with a total of 12 detectors, four between the beryllium target and the magnetic field and four pairs behind the field to measure the two separated beams. We dispose the detectors at constant intervals of 2 m leaving 1 m between the magnetic field region and the closest detectors for an overall length of 18 m. Figure 12 shows the positions where particle will intersect detectors.

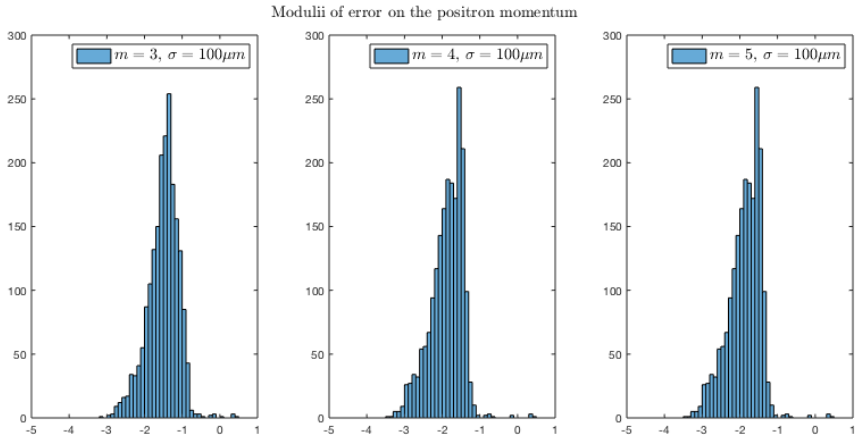

Figure 11: ϵ distribution for different number of detectors

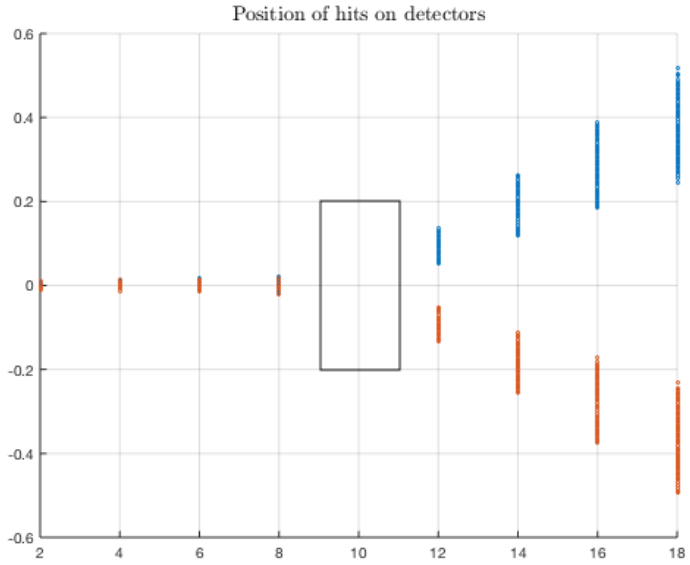

Figure 12: Positions of the detectors before and after the magnetic field.

3.6 Detectors' sizes

To estimate the required size of the detectors, we consider the worst case scenario where produced muons are generated with all their momenta parallel to the x-axis (CM frame). In this case

$$p^* = \sqrt{\frac{s}{4} - m_\mu^2} \simeq \sqrt{\frac{m_e E}{2} - m_\mu^2} = p_x \ , \tag{27}$$

where we used $s \simeq 2m_e E$, with $E = 49GeV$ the nominal energy and the obvious fact that p_x is not changed by a boost orthogonal to its direction. Along the z axis we have, instead,

$$p_z = \gamma\beta E^* = \frac{E}{2}\sqrt{1 - \frac{m_e}{2E}} \ . \tag{28}$$

The maximum angle between the direction of motion of the emerging muon pairs and the direction of motion of the incident positron is

$$\tan\theta_M = \frac{p_x}{p_y} = \frac{2}{E}\sqrt{\frac{E(m_e E - 2m_\mu^2)}{2E - m_e}} \simeq \frac{\sqrt{2m_e E - 4m_\mu^2}}{E} \simeq 1.9 \cdot 10^{-3}, \quad (29)$$

thus

$$\theta_M \simeq 0.11^\circ. \quad (30)$$

If the last detector before the region with magnetic field is at $\sim 10m$, in order to have a 100% acceptance rate, the diameter of the detector at has to be $\sim 4cm$.
Due to the uncertainty on the initial momentum of the particles, an estimate of the upper bound on the size of the detectors to be placed after the magnetic fields is too complex, so we simulated 10000 events and plotted the hits on a detector placed at $18m$ from the block of beryllium and at $7m$ from the end of the magnetic field.

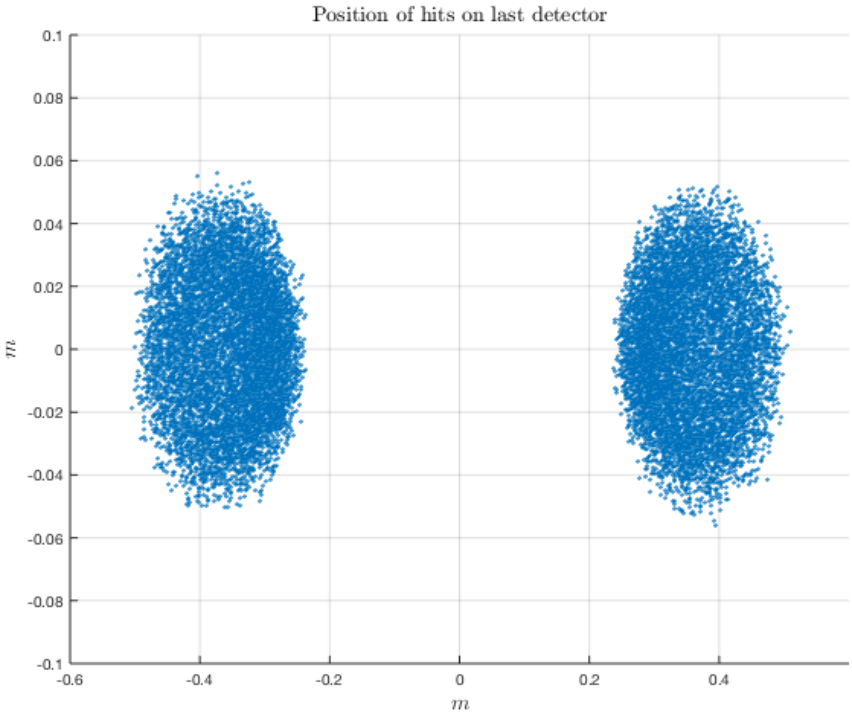

Figure 13: Hits on the last detector after the magnetic field, as a section of the xy plane.

As shown in Figure 13, in order to have 100% acceptance one would need detectors of size approximately $35 \times 12cm$. In order to reduce the size of the detectors in the x direction one could reduce either the intensity or the length of the magnetic field.

Now, we simulated ≥ 10000 hits on a detector at $1m$ from the beryllium block (as a worst-case scenario) and plotted the distribution of the distance between two hits.

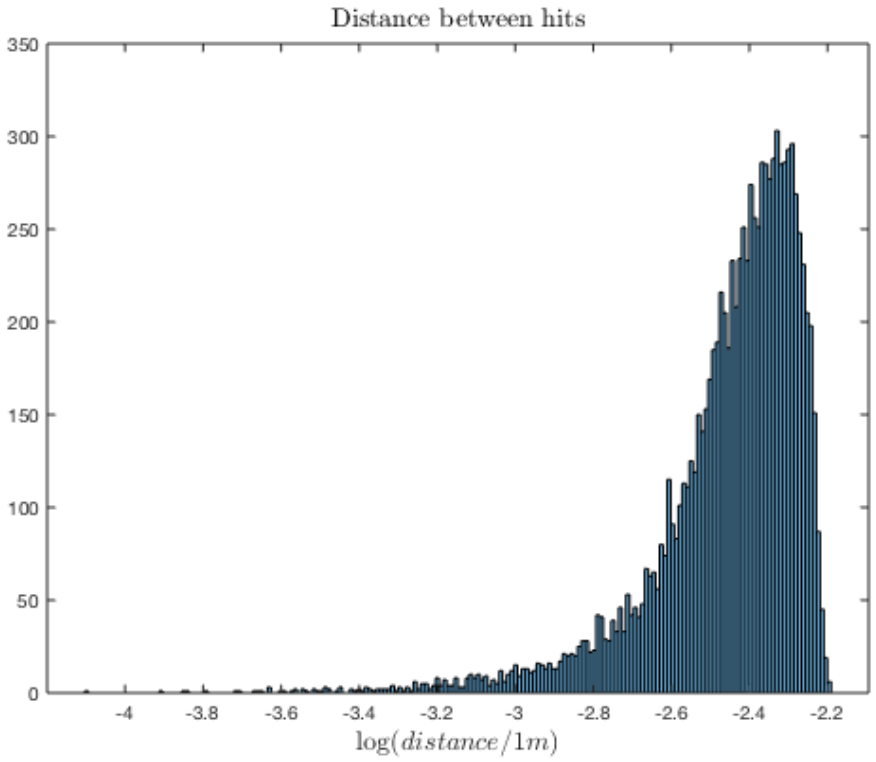

Figure 14

As shown in Figure 14, the great majority of the pairs of hits has pairwise distance greater than $10^{-3}m$, while less than one in 10^4 events has pairwise distance smaller than $10^{-4}m$, which is the typical resolution of the detectors. When considering the hits on the last detector, which realistically is placed at $\sim 10m$, the probability of having two hits closer than the resolution of the detector is practically zero. As described in Section 3.2, the tracking algorithm only needs one detector to recognize two distinct hits to output two distinct trajectories: even in the case that the first detectors were unable to distinguish between two hits the software would still produce a correct answer.
Finally, we aim at evaluating how the uncertainty σ on the hits on the detectors affects the final result. From Figure 15 we can see that halving σ translates the distribution of ϵ to the left for a constant distance so we can hypnotize a linear relation between σ and the relative error.

To calculated the resolution of the system on the measurement of the invariant mass $\sqrt{s}$ we generated a set of events with the same real total momentum. We then compute the resolution from the distribution of measured values as the ratio of the full wide at half maximum over the true value

$$R = \frac{FWHM}{\sqrt{s}} \approx \frac{2.355\sigma_{\sqrt{s}}}{\sqrt{s}} \approx 0.09\% \tag{31}$$

where $\sigma_{\sqrt{s}}$ is the standard deviation that we obtain from a fit of the peak of the distribution shown in Figure 16

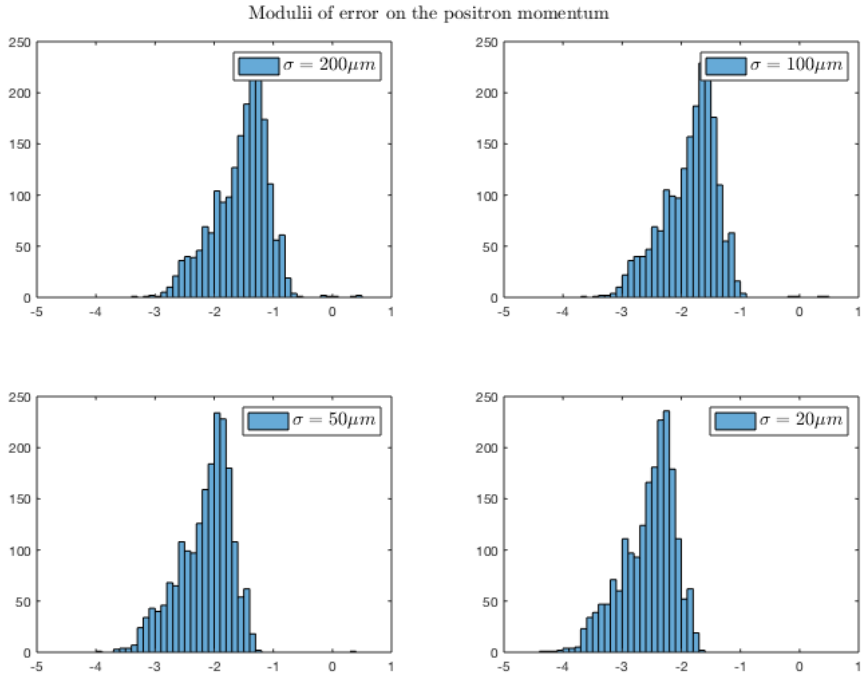

Figure 15: ϵ distribution for different resolution of detectors

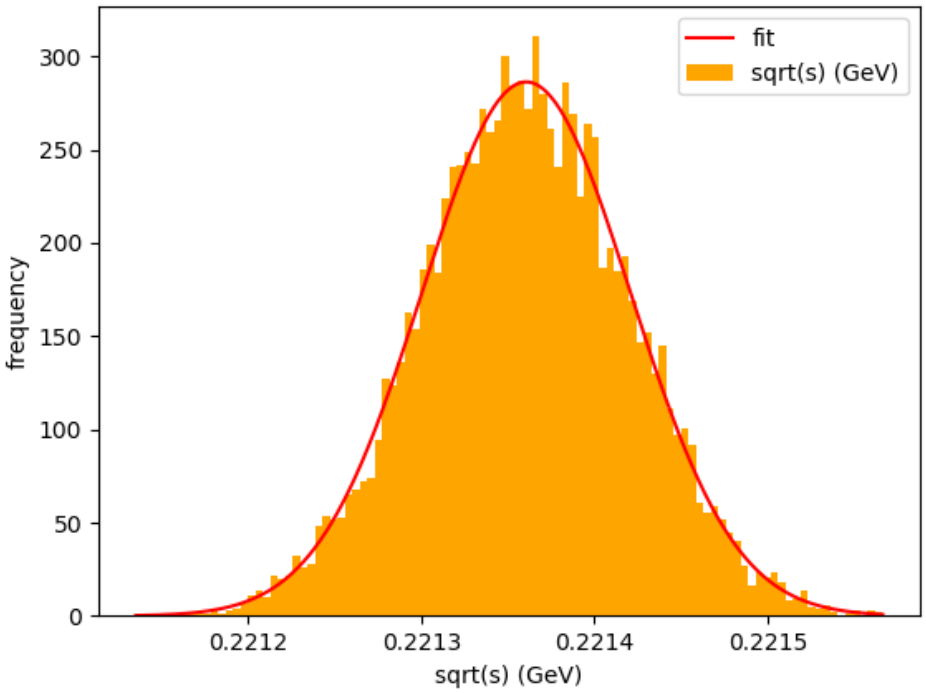

Figure 16: $\sqrt{s}$ distribution for a fixed initial momentum